Deep-ultraviolet surface plasmon resonance of Al and Al_{core}/Al_2O_{3shell} nanosphere dimers for surface-enhanced spectroscopy*

Ci Xue-Ting(慈雪婷), Wu Bo-Tao(吴伯涛)†, Song Min(宋 敏), Chen Geng-Xu(陈耿旭), Liu Yan(刘 岩), Wu E(武 愕), and Zeng He-Ping(曾和平)‡

State Key Laboratory of Precision Spectroscopy, East China Normal University, Shanghai 200062, *China*

(Received 29 February 2014; revised manuscript received 24 March 2014; published online 23 July 2014)

The localized surface plasmon resonance properties of Al and Al_{core}/Al_2O_{3shell} nanosphere dimers with Al and Al core nanosphere radii of 20 nm and Al_2O_3 shell of 2 nm in the deep-ultraviolet region have been studied using the finite difference time domain method. The extinction spectra and the electric field distribution profiles of the two dimers for various gap distances between two individual nanospheres are compared with those of the corresponding monomers to reveal the extent of plasmon coupling. It is found that with the interparticle distance decreasing, a strong plasmon coupling between two Al or Al_{core}/Al_2O_{3shell} nanospheres is observed accompanied by a significant red shift in the extinction spectra at the parallel polarization direction of the incident light related to the dimer axis, while for the case of the perpendicular polarization direction, a weak plasmon coupling arises characterized by a slight blue shift in the extinction spectra. The electric field distribution profiles show that benefiting from the dielectric Al_2O_3 shell, the gap distance of Al_{core}/Al_2O_{3shell} nanosphere dimers can be tailored to < 1 nm scale and results in a very high electric field enhancement. The estimated surface-enhanced Raman scattering enhancement factors suggests that the Al_{core}/Al_2O_{3shell} nanosphere dimers with the gap of < 1 nm gave rise to an enhancement as high as 8.1×10^7 for interparticle gap = 0.5 nm. Our studies reveal that the Al_{core}/Al_2O_{3shell} nanosphere dimers may be promising substrates for surface-enhanced spectroscopy in the deep-ultraviolet region.

Keywords: localized surface plasmon resonance, deep ultraviolet, aluminum nanosphere dimers, enhanced spectroscopy

PACS: 73.20.MF, 78.67.–n, 78.67.Bf, 78.20.Bh **DOI:** 10.1088/1674-1056/23/9/097303

1. Introduction

Localized surface plasmon resonance (LSPR) in metallic nanostructures originates from the collective oscillation of free conduction electrons in metal surface when interacting with light, which is highly sensitive to the metal composition, shape, size, and surrounding environment.[1,2] Due to the high ability to enhance and concentrate electric fields down to nanometer scale, LSPR of metallic nanostructures has a wide range of applications in plasmonic photovoltaic cells,[3] surface-plasmon enhanced spectroscopies,[4–8] photochemistry,[9,10] sensing,[11,12] photodetectors,[13] and quantum optics.[14–16] Plasmonic properties in these applications were usually carried out with noble metals Au and Ag, where LSPR is limited in the visible and near-infrared (NIR) light regions due to damping in the ultraviolet (UV) and deep-ultraviolet (DUV) regions caused by the interband transitions. However, there is an increasing interest in extending LSPR to the UV and DUV regions. UV and DUV plasmons have potential advantage in application of Raman spectroscopy for many organic and inorganic molecules with small Raman cross sections in the visible and NIR regions,[17] as well as many important biomolecules, such as DNA and proteins, which have their electronic absorption bands in the DUV region.[18] Furthermore, UV and DUV excitations can well separate the fluorescence and Raman bands and accordingly lead to a fluorescence-free background, and thus largely improve the signal-to-noise ratio of Raman spectra.[19]

In order to obtain plasmon resonance in the UV and DUV regions, many metals, such as Al, Ga, In, Tl, Pb, and Bi, have been theoretically explored.[20] However, to achieve strong and long-lived UV and DUV plasmons, it is necessary for a metal to have a negative dielectric constant and a minimal loss coefficient in the UV and DUV regions. Al is thought to be the best and probably the only choice of metal that meets this criterion. The LSPR properties of Al nanostructures as well as their applications in UV and DUV Raman spectroscopy, enhanced UV fluorescence and nonlinear plasmonics have been demonstrated in several geometries, including spheres,[21–23] discs,[24,25] triangles,[26–28] and rods.[21,23,29–31] It is well known that when metal nanoparticles are brought in proximity, LSPR in individual particles couples to each other and forms new optical modes by plasmon hybridization.[32] Plasmon coupling has been found to give rise to a more profound plasmon resonance than that

*Project supported by the National Natural Science Foundation of China (Grant Nos. 11104079 and 61378033), the National Key Scientific Instrument Project of China (Grant No. 2012YQ150092), the Research Foundation for the Doctoral Program of Higher Education of China (Grant No. 20110076120019), and the State Key Laboratory of Luminescent Materials and Devices at South China University of Technology.

†Corresponding author. E-mail: btwu@phy.ecnu.edu.cn

‡Corresponding author. E-mail: hpzeng@phy.ecnu.edu.cn

© 2014 Chinese Physical Society and IOP Publishing Ltd

in isolated particles. For example, the near-field enhancements in the vicinity of dimers, trimers, and oligomers of metal particles are much higher than those of the corresponding monomers.[33–35] In the case of Al, there has been very limited literature about the LSPR properties of Al hybridized nanostructures so far.[22,28,31]

In this paper, we present a theoretical study on the interaction of electromagnetic radiation with Al nanosphere dimers using the finite difference time domain (FDTD) method. Dimeric Al nanospheres are constructed by individual monomers with a radius of 20 nm. Optical features of Al spherical dimers with various surface-to-surface distances, $d = 3$, 5, 10, 20, 30, and 40 nm are examined in the DUV region. The simulations are also performed to investigate the influence of Al_2O_3 shell formed on the surface of Al nanospheres due to oxidation in air on the LSPR of Al nanosphere dimers. Finally, the potential applications of Al_{core}/Al_2O_{3shell} nanosphere dimers in surface-enhanced Raman scattering (SERS) are evaluated.

2. Theoretical method

Numerical simulations were performed using the FDTD solutions software (version 8.5, Lumerical Solution, Inc. Canada). Figure 1 shows the schematic diagrams of the Al and Al_{core}/Al_2O_{3shell} nanosphere dimers performed in the simulations. In FDTD method, Maxwell's equations are solved numerically on discrete grids involving space and time. The method is based on the Yee algorithm, in which the derivatives involving space and time are replaced by the finite differences, and the electric and magnetic fields are evaluated on grids that are interspersed both in space and time. A dielectric function $\varepsilon(\omega)$ is used to represent the metallic system of interest. Here we use Palik's bulk dielectric data for Al and Al_2O_3 from Ref. [36], and a vacuum is chosen to be the background medium with a refractive index of 1.0. A plane wave total field-scattered field (TFSF) source with a wavelength range 100–600 nm is utilized as the incident light beam. The amplitude of the electric field of the incident light is taken to be 1.0 V/m. We use a set of power monitors to calculate the net power flowing into the total and scattered field simulation locations and estimate the absorption and scattering cross sections. The sum of both the above cross sections gives the extinction cross section. The electric field distribution in the vicinity of nanosphere dimers is evaluated using the frequency domain field profile monitors. We use perfectly matched layer (PML) absorption boundary conditions as well as symmetric and anti-symmetric boundary conditions to reduce the memory requirement and computational time. In all the simulations, a three-dimensional nonuniform meshing is used, and grid sizes of 0.5 nm and 0.125 nm for interparticle gap > 1 nm and ≤ 1 nm respectively are chosen for the inside and immediate vicinity of Al or Al_{core}/Al_2O_{3shell} nanosphere dimers. To reduce the simulation error, the careful and systematic convergence tests of the simulation data were performed.

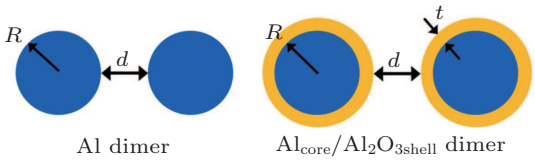


Fig. 1. (color online) Schematic of Al and Al_{core}/Al_2O_{3shell} nanosphere dimers. The R is the Al or Al core nanosphere radius, t is the thickness of Al_2O_3 shell, and d is the interparticle distance.

3. Results and discussion

It has been shown that LSPR properties of metal nanostructures were sensitive to their surrounding environment.[1,2] In our simulation, LSPR peaks of Al and Al_{core}/Al_2O_{3shell} nanosphere dimers produced a slight red shift of several nanometers when placed on quartz substrates and exhibited a large red shift of several tens nanometers when changing the background medium from vacuum to water. Here, for simplicity we investigated LSPR properties of Al and Al_{core}/Al_2O_{3shell} nanosphere dimers without considering substrate effects and using a vacuum as the background medium. Optical extinction spectra of spherical Al dimers (with $R = 20$ nm nanospheres as the monomers) as a function of the interparticle distance ($d = 3$–40 nm) at the parallel and perpendicular polarization directions of the incident light related to the dimer axis are shown in Fig. 2. The monomer spectra are also included for comparison. For the $R = 20$ nm Al nanosphere monomer, its extinction spectrum shows a λ_{max} at about 186 nm with a shoulder at about 158 nm, which originates from dipole and quadrupole resonances of Al nanosphere, respectively.[21–23] It can also be found that the extinction spectra are the same for the parallel and perpendicular polarization directions due to its symmetrical shape. For the dimers, an apparent red shift of the dipole resonance λ_{max} for the parallel polarization while a slight blue shift for the perpendicular polarization with the gap size d decreasing can be clearly seen in comparison with the monomer bands. The spectral shifts occur because the magnitude of plasmon coupling between two individual Al nanospheres increases with the decrease of interparticle distance. Although the $R = 20$ nm Al nanosphere exhibits a quadrupole resonance, the extinction spectra for the parallel polarization in Fig. 2(a) are mainly dominated by the plasmon coupling of the dipole resonances from two monomers due to the weak quadrupole resonances. Therefore the optical modes in the dimers can still be described using the plasmon hybridization model. The dimeric plasmon modes, deriving from the eigenmodes belonging to the two individual monomers can be viewed as bonding and antibonding combinations evolving into lower and higher energies, as shown in Fig. 3.[32] The different optical responses of bonding and antibonding modes to the polarization of incident light will lead

to red or blue shifts of the resonance peaks, and the shift extent depends on the extent of plasmon coupling. In the dimer, the bonding mode for the parallel polarization excitation gives rise to a strong plasmon coupling between two monomeric Al nanospheres and thus leads to a significant red shift. On the contrary, the slight blue shift for the excitation of antibonding mode at the perpendicular polarization is a result of weak plasmon coupling. As the gap size $d = 40$ nm, the extinction spectra for the parallel and perpendicular polarizations almost recover that of the monomer, meaning that the plasmon coupling between the two Al nanospheres can be negligible at this separation and beyond.

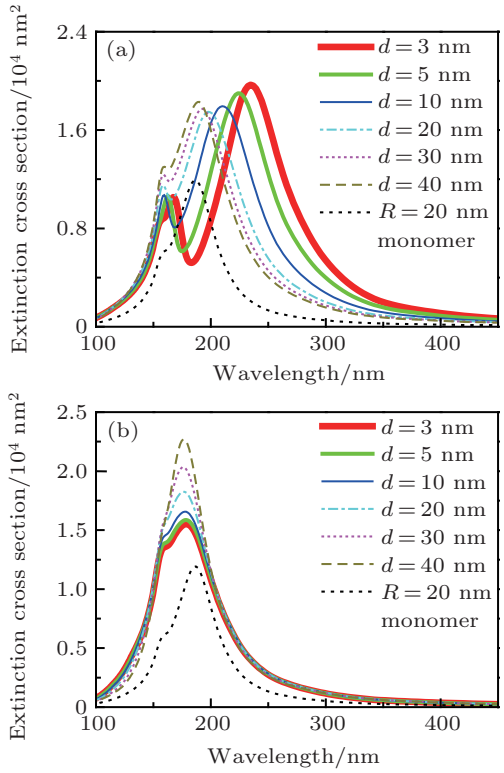


Fig. 2. (color online) Extinction spectra of Al nanosphere dimers dependent on gap distance d for the parallel (a) and perpendicular (b) polarizations of the incident light related to the dimer axis.

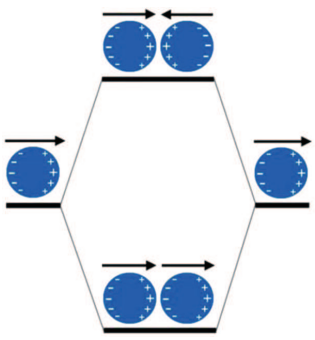


Fig. 3. (color online) Schematic of plasmon coupling in Al nanosphere dimers for the parallel polarization of the incident light.

In the classical electromagnetic coupling regime, the dipole resonance $\lambda_{\max}$ for dimers at the parallel polarization of the incident light obeys the plasmon rule equation proposed by El-Sayed and co-workers,[37] which is particularly useful to illustrate the universal scaling behavior of plasmon coupling since this relationship is particle size, shape, metal type and medium dielectric constant invariant. The ratio of resonance wavelength shift $\Delta\lambda$ to monomer resonance wavelength λ_0 follows an exponential dependence on the ratio of interparticle separation d to particle diameter D given by

$$\Delta\lambda/\lambda_0 = A\,\mathrm{e}^{-(d/D)/\tau} + C, \tag{1}$$

where $\Delta\lambda$ denotes the resonance wavelength shift with respect to the monomer resonance wavelength λ_0, τ is the decay constant, and A and C are two constants. The simulation extinction data of the dimer and the corresponding fit to the plasmon rule equation are shown in Fig. 4. The τ value for Al nanosphere dimers is 0.22 ± 0.02, in excellent agreement with those of Au nanoparticle dimers.[34,37]

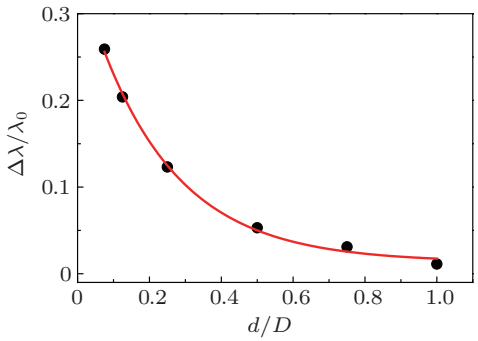


Fig. 4. (color online) Experimental fractional plasmon shift versus the ratio of interparticle gap to nanosphere diameter, which can be fit to a single exponential decay (solid red curve).

The electric field intensity distribution profiles in the vicinity of Al nanosphere dimers for various d at their $\lambda_{\max}$ are illustrated in Fig. 5 for the parallel polarization of the incident light. The $|E|^2/|E_0|^2$ values on the surface of Al nanospheres at the junctions of the dimers are the highest when $d = 3$ nm, and then decreases with the increase of d. Those regions with enhanced electric field at the junctions are well known as hot spots,[38,39] and can be clearly observed from the field contours in Fig. 5. For the case of the perpendicular polarization of the incident light, the field profiles at their $\lambda_{\max}$ exhibit a close invariant dependence on the separation distance d and behave like two isolated monomers rather than as a single dimer (see Fig. 6), which is due to the weak plasmon coupling between two Al nanospheres when the incident light polarization is perpendicular to the dimer axis. Furthermore, it can be seen apparently that the longitudinal plasmon coupling shows much stronger in comparison with that of the transverse coupling, and accordingly the electric field intensity for the parallel polarization is much higher than that for the perpendicular polarization.

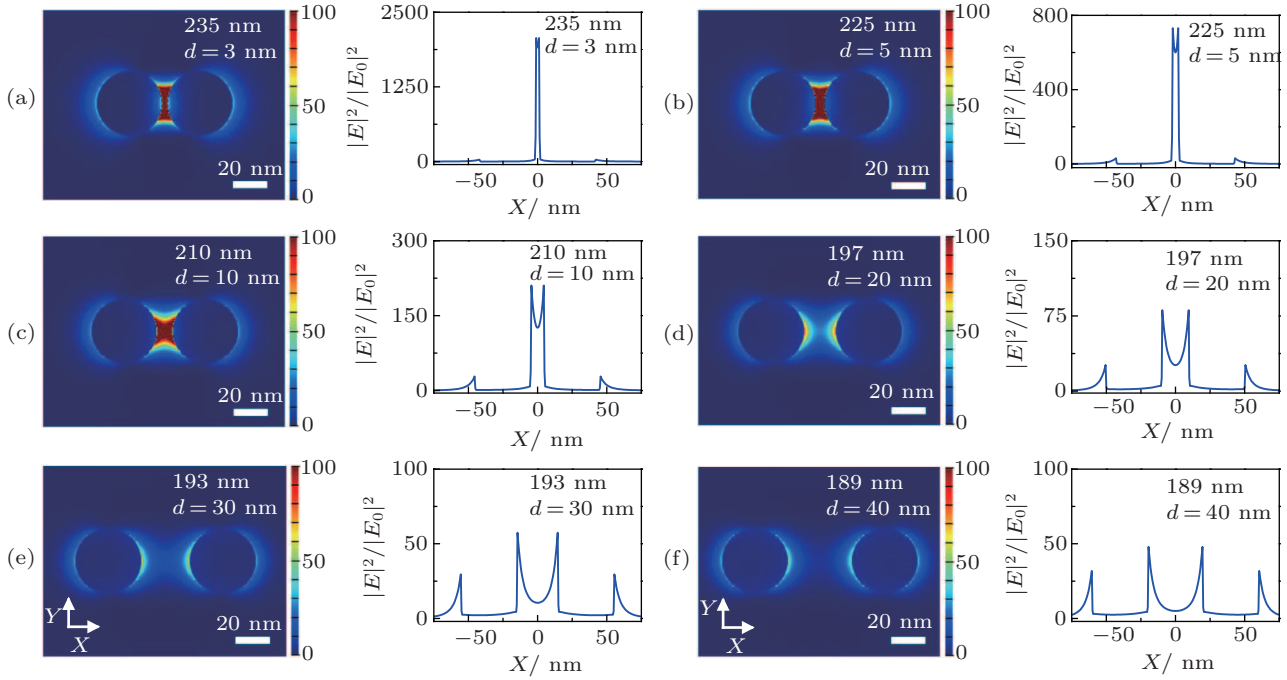


Fig. 5. (color online) Electric field intensity distribution profiles in the vicinity of Al nanosphere dimers at their λ_{max} as a function of the gap distance d for the parallel polarization of the incident light. (a) $\lambda_{max} = 235$ nm, $d = 3$ nm; (b) $\lambda_{max} = 225$ nm, $d = 5$ nm; (c) $\lambda_{max} = 210$ nm, $d = 10$ nm; (d) $\lambda_{max} = 197$ nm, $d = 20$ nm; (e) $\lambda_{max} = 193$ nm, $d = 30$ nm; (f) $\lambda_{max} = 189$ nm, $d = 40$ nm.

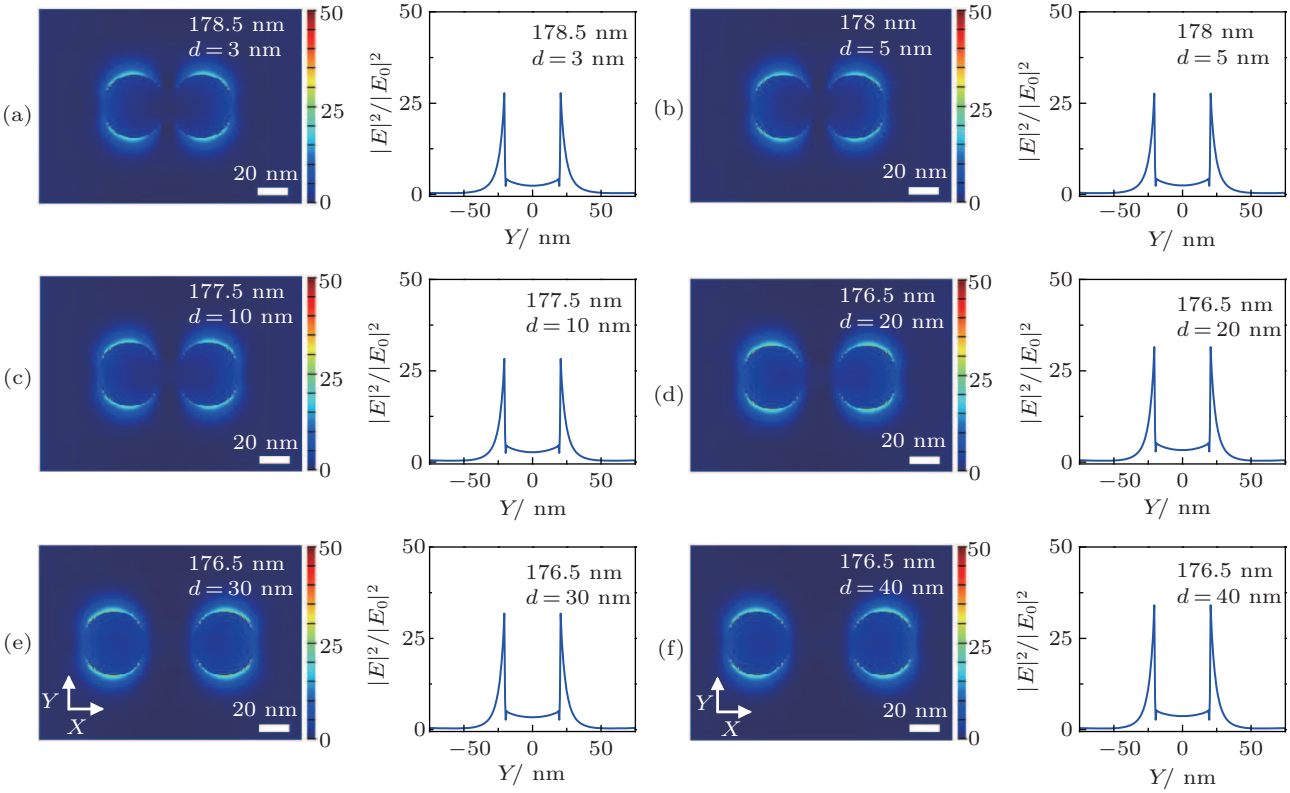


Fig. 6. (color online) Electric field intensity distribution profiles in the vicinity of Al nanosphere dimers at their λ_{max} as a function of the gap distance d for the perpendicular polarization of the incident light. (a) $\lambda_{max} = 178.5$ nm, $d = 3$ nm; (b) $\lambda_{max} = 178$ nm, $d = 5$ nm; (c) $\lambda_{max} = 177.5$ nm, $d = 10$ nm; (d) $\lambda_{max} = 176.5$ nm, $d = 20$ nm; (e) $\lambda_{max} = 176.5$ nm, $d = 30$ nm; (f) $\lambda_{max} = 176.5$ nm, $d = 40$ nm.

When Al nanostructures are exposed in the ambient air, there will be a natural and stable Al_2O_3 oxidation layer about 2–3 nm forming on the surface,[21,26] which acts as a passive and protective layer against environmental degradation. To explore the influence of the oxide layer on the plasmon response of Al spherical dimers, we introduced Al_{core}/Al_2O_{3shell} nanosphere dimers in our simulations with the Al core radius of 20 nm and a fixed Al_2O_3 shell thickness of 2 nm[26,27] but with different gap distances between the two core–shell nanospheres. The surface-to-surface gap d varies from 0 to

6 nm, i.e., the surface-to-surface distance between two Al nanosphere cores varies from 4 nm to 10 nm. The extinction spectra at the parallel and perpendicular polarizations of the incident light as a function of the d are shown in Fig. 7. As earlier seen in Fig. 2, the extinction spectra of Al_{core}/Al_2O_{3shell} nanosphere dimers also show a large red shift for the parallel polarization and a slight blue shift for the perpendicular polarization until the d decreases to 0 nm compared with that of the corresponding monomer. In a metallic dimer system interacting with the parallel polarization light, it was known that a red shift of the LSPR band was typically observed while decreasing the interparticle distance due to the hybridization of two individual particle plasmons, but a blue shift in the LSPR band could be observed when electron tunneling effect or charge transfer plasmon began to be present as further decreasing the interparticle distance down to < 1 nm.[40,41] In our case, the surface of Al nanospheres is coated with a 2-nm layer of dielectric Al_2O_3, which is transparent from the DUV to visible-light regions.[23,26] Thus, when the interparticle gap between two Al_{core}/Al_2O_{3shell} core–shell nanospheres decreases down to 0 nm, the electron tunneling effect or charge transfer plasmon still cannot occur because the actual distance between two metallic Al cores is at least no smaller than 4 nm. The electric field intensity distribution profiles in the vicinity of Al_{core}/Al_2O_{3shell} nanosphere dimers as a function of the d at their λ_{max} for the parallel polarization of the incident light are illustrated in Fig. 8. Except the case of $d = 0$ nm, the hot spots all arise in the junctions of the dimers along the dimer axis, and the electric field enhancement factor rapidly decreases with the gap d increasing. When two core–shell nanospheres touch ($d = 0$ nm), the hot spot is not in the junction along the dimer axis due to the gap absence, while it is interesting to find that two hot spots symmetrically occur in the gaps near the touching point of Al_2O_3 shells along the perpendicular direction. However, owing to these gaps deviating from the junction point, the surface charge accumulation in these gap surfaces may be lower than that in the junction of core–shell dimer with $d = 0.5$ nm, and thus the maximum near field enhancement for core–shell dimer with $d = 0$ nm is smaller than that with $d = 0.5$ nm. Comparing Fig. 5 with Fig. 8, it is also noticed that the electric field enhancement in Al_{core}/Al_2O_{3shell} nanosphere dimers is more pronounced and efficient than that in Al nanosphere dimers, even though they have the same distance between two Al metal nanospheres, such as Al nanosphere dimer with $d = 5$ nm and Al_{core}/Al_2O_{3shell} nanosphere dimer with $d = 1$ nm, which can be explained as follows. Light enhancement and confinement in metal dimeric nanostructures is caused by the discontinuity of the electric field at the gap interfaces.[42] The refractive index of Al_2O_3 is higher than that of Al, thus when the gap interface changes from Al-air in Al nanosphere dimer to Al_2O_3-air in Al_{core}/Al_2O_{3shell} nanosphere dimer the discontinuity of the electric field at Al_2O_3–air interfaces becomes larger compared with that at Al-air interfaces, and concomitantly light enhancement and confinement is increased. Furthermore, as a direct consequence of the boundary conditions, the dominating field components normal to the gap interfaces are sizable only inside the gap. This means that the achievable field confinement is not limited by the skin depth of the metal, but is solely determined by the actual size of the gap.[43] Al_2O_3 shells reduce the gap from 5 nm in Al nanosphere dimer to 1 nm in Al_{core}/Al_2O_{3shell} dimer, and thus Al_{core}/Al_2O_{3shell} dimer has a stronger field confinement than Al nanosphere dimer. For the gap interfaces with high-index contrast and small gap, Al_{core}/Al_2O_{3shell} dimer shows a strong near field enhancement compared with Al dimer, although they have the same distance between two Al metal nanospheres. For the perpendicular polarization of the incident light, the field profiles at the λ_{max} exhibit a similar tendency as the case of Al nanosphere dimers without oxidation layers (Fig. 6). The field profiles have a close invariant dependence on the separation distance d and behave as two isolated monomers rather than as a dimer due to the weak plasmon coupling between two Al_{core}/Al_2O_{3shell} core–shell nanospheres (data not shown). In the same way, the longitudinal plasmon coupling is also much stronger than the transverse one.

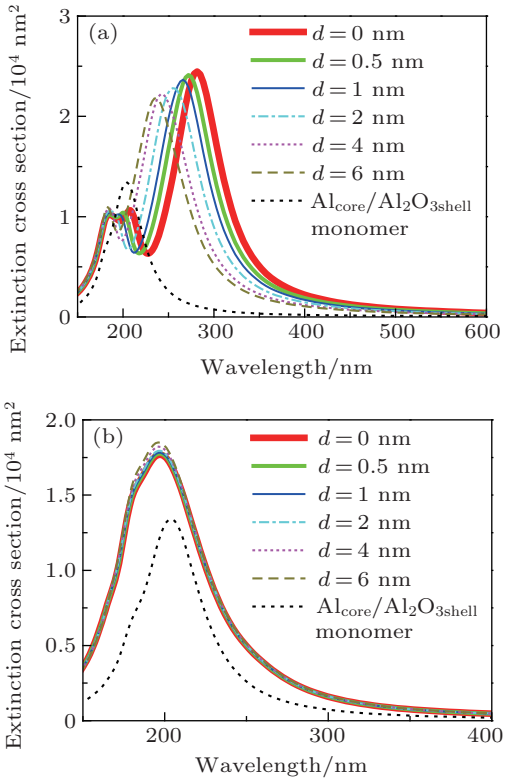


Fig. 7. (color online) Extinction spectra of Al_{core}/Al_2O_{3shell} core–shell nanosphere dimers dependent on gap distance d for the parallel (a) and perpendicular (b) polarizations of the incident light related to the dimer axis.

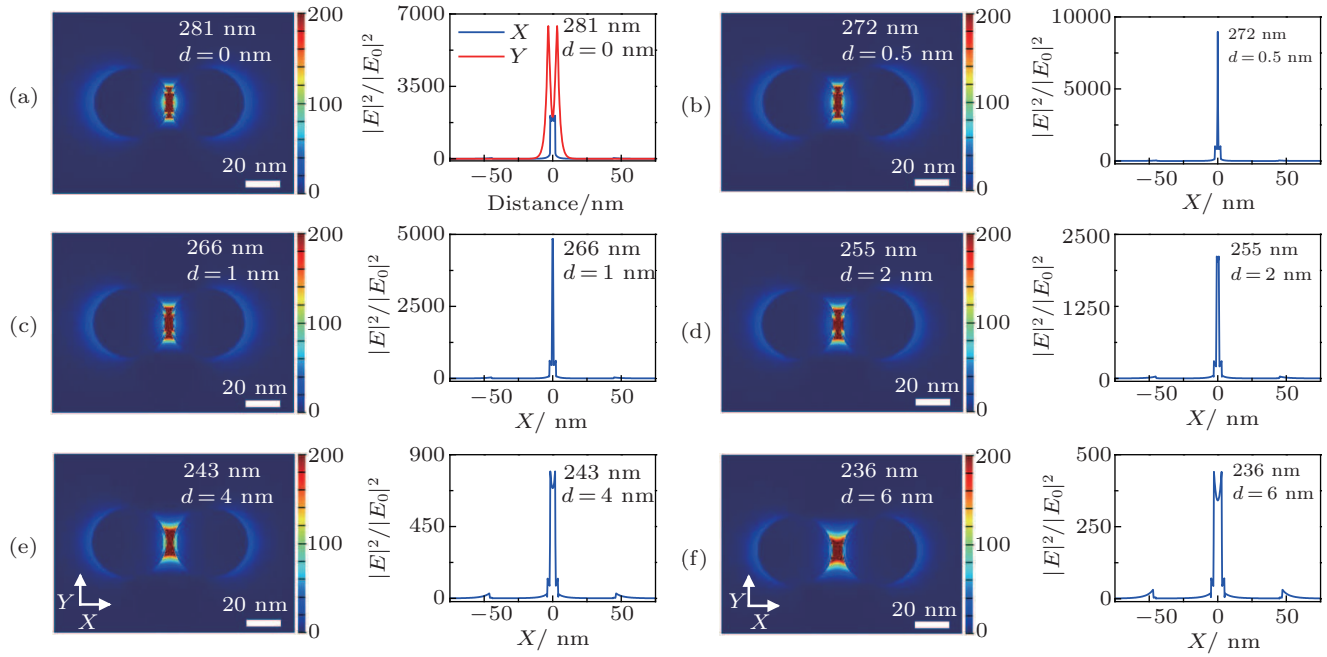


Fig. 8. (color online) Electric field intensity distribution profiles in the vicinity of Al_{core}/Al_2O_{3shell} core–shell nanosphere dimers at their λ_{max} as a function of the gap distance d for the parallel polarization of the incident light. (a) $\lambda_{max} = 281$ nm, $d = 0$ nm; (b) $\lambda_{max} = 272$ nm, $d = 0.5$ nm; (c) $\lambda_{max} = 266$ nm, $d = 1$ nm; (d) $\lambda_{max} = 255$ nm, $d = 2$ nm; (e) $\lambda_{max} = 243$ nm, $d = 4$ nm; (f) $\lambda_{max} = 236$ nm, $d = 6$ nm.

The interparticle distance in metal dimeric nanostructures plays a crucial role in obtaining a high electric field enhancement. It has been reported that controlling < 1 nm plasmonic gap in metallic dimers was especially important because the plasmon coupling intensity increased exponentially within this gap distance.[44,45] However, based on the quantum mechanical calculations, it was reported that for the metal dimer separations below 1 nm, electron tunneling across the dimer junction or charge transfer plasmon can drastically reduce the electric field enhancement relative to classical predictions.[46,47] Benefiting from the dielectric Al_2O_3 layer, the two nanospheres of the Al_{core}/Al_2O_{3shell} core–shell nanosphere dimers can approach very close without considering the electron tunneling effect across the dimer junction or charge transfer plasmon. Accordingly, the electric field can be extremely concentrated and localized in a very small volume by carefully tailoring the interparticle distance, and concomitantly a very high electric field enhancement can be achieved. As seen in Fig. 8, with the gap decreasing within 1 nm, the electric field enhancement factor steeply increases, and when the gap is 0.5 nm an electric field enhancement factor up to 9×10^3 is obtained. Such a high near field enhancement in the DUV region is very useful for surface-enhanced Raman scattering (SERS), because the SERS enhancement factor approximately has a fourth power dependence on the incident electric field intensity in SERS scales. The SERS enhancement factors as a function of the interparticle gap distance at the plasmon resonance λ_{max} are shown in Fig. 9. It is seen that the SERS enhancement factor rapidly increases when the gap is < 1 nm. The maximum SERS enhancement factor is about 8.1×10^7 (for gap = 0.5 nm), which is large enough even for single-molecule level detection. To the best of our knowledge, no SERS experiments have been carried out on Al_{core}/Al_2O_{3shell} nanosphere dimers that we report in this manuscript, and we hope that our study can motivate experiments in this direction.

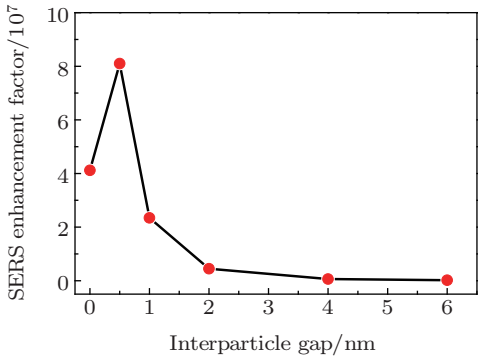


Fig. 9. (color online) SERS enhancement factor as a function of interparticle gap.

4. Conclusion

In summary, we have investigated optical extinction properties in the DUV region and electric field intensity distribution patterns of Al and Al_{core}/Al_2O_{3shell} nanosphere dimers using the FDTD method. The Al and Al core nanospheres in dimers had the same radius of 20 nm and the thickness of Al_2O_3 shell was fixed at 2 nm. It was found that with the increasing interparticle distance d, the extinction spectra of the Al and Al_{core}/Al_2O_{3shell} nanosphere dimers all exhibited a red shift for the parallel polarization and a slight blue shift for the perpendicular polarization compared with those of the corresponding monomers. The electric field intensity distribution patterns revealed that benefiting from the dielectric

Al_2O_3 shell, the gap distance of Al_{core}/Al_2O_{3shell} nanosphere dimers could be tailored to < 1 nm scale and accordingly very high EF enhancements were obtained compared with the case of Al nanosphere dimers. The potential application of Al_{core}/Al_2O_{3shell} nanosphere dimers in SERS was evaluated and the maximum SERS enhancement factor was up to 8.1×10^7 (for interparticle gap = 0.5 nm). Our studies prove that the Al_{core}/Al_2O_{3shell} nanosphere dimers have potential applications in surface-enhanced spectroscopy in the DUV region, solar cell and UV optical lithography.

References

[1] Kelly K L, Coronado E, Zhao L L and Schatz G C 2003 *J. Phys. Chem. B* **107** 668
[2] Tao J, Lu Y H, Zheng R S, Lin K Q, Xie Z G, Luo Z F, Li S L, Wang P and Ming H 2008 *Chin. Phys. Lett.* **25** 4459
[3] Atwater H A and Polman A 2010 *Nat. Mater.* **9** 205
[4] Kinkhabwala A, Yu Z, Fan S H, Avlasevich Y, Muellen K and Moerner W E 2009 *Nat. Photonics* **3** 654
[5] Wu E, Chi Y Z, Wu B T, Xia K W, Yokota Y, Ueno K, Misawa H and Zeng H P 2011 *J. Lumin.* **131** 1971
[6] Yokota Y, Ueno K and Misawa H 2011 *Chem. Commun.* **47** 3505
[7] Song M, Chen G X, Liu Y, Wu E, Wu B T and Zeng H P 2012 *Opt. Express* **20** 22290
[8] Li J F, Huang Y F, Ding Y, Yang Z L, Li S B, Zhou X S, Fan F R, Zhang W, Zhou Z Y, Wu D Y, Ren B, Wang Z L and Tian Z Y 2010 *Nature* **464** 392
[9] Ueno K, Juodkazis S, Shibuya T, Yokota Y, Mizeikis V, Sasaki K and Misawa H 2008 *J. Am. Chem. Soc.* **130** 6928
[10] Wu B T, Ueno K, Yokota Y, Sun K, Zeng H P and Misawa H 2012 *J. Phys. Chem. Lett.* **3** 1443
[11] Zhao H J 2012 *Chin. Phys. B* **21** 087104
[12] Zhang Z Y, Wang L N, Hu H F, Li K W, Ma X P and Song G F 2013 *Chin. Phys. B* **22** 104213
[13] Wang X M, Song M, Liang Y, Wang Z Y, Kong W B, Huang J H, Wu E, Wu B T, Wu G and Zeng H P 2013 *Opt. Express* **21** 6442
[14] Akimov A V, Mukherjee A, Yu C L, Chang D E, Zibrov A S, Hemmer P R, Park H and Lukin M D 2007 *Nature* **450** 402
[15] Chi Y Z, Chen G X, Jelezko F, Wu E and Zeng H P 2011 *IEEE Photon. Technol. Lett.* **23** 374
[16] Chen G X, Liu Y, Song M, Wu B T, Wu E and Zeng H P 2013 *IEEE J. Sel. Top. Quant.* **19** 4602404
[17] Efremov E V, Ariese F and Gooijer C 2008 *Anal. Chim. Acta* **606** 119
[18] Asher S A 1993 *Anal. Chem.* **65** 59A
[19] Asher S A and Johnson C R 1984 *Science* **225** 311
[20] McMahon J M, Schatz G C and Gray S K 2013 *Phys. Chem. Chem. Phys.* **15** 5415
[21] Ekinci Y, Solak H H and Löffler J F 2008 *J. Appl. Phys.* **104** 083107
[22] Chowdhury M H, Ray K, Gray S K, Pond J and Lakowicz J R 2009 *Anal. Chem.* **81** 1397
[23] Hu J L, Chen L, Lian Z C, Cao M, Li H J, Sun W B and Tong N L 2012 *J. Phys. Chem. C* **116** 15584
[24] Langhammer C, Schwind M, Kasemo B and Zoric I 2008 *Nano Lett.* **8** 1461
[25] Jha S K, Ahmed Z, Agio M, Ekinci Y and Löffler J F 2012 *J. Am. Chem. Soc.* **134** 1966
[26] Chan G H, Zhao J, Schatz G C and Duyne R P V 2008 *J. Phys. Chem. C* **112** 13958
[27] Taguchi A, Saito Y, Watanabe K, Song Y J and Kawata S 2012 *Appl. Phys. Lett.* **101** 081110
[28] Li L, Lim S F, Puretzky A A, Riehn R and Hallen H D 2012 *Appl. Phys. Lett.* **101** 113116
[29] Castro-Lopez M, Brinks D, Sapienza R and Hulst N F 2011 *Nano Lett.* **11** 4674
[30] Knight M W, Liu L F, Wang Y M, Brown L, Mukherjee S, King M S, Everitt H O, Nordlander P and Halas N J 2012 *Nano Lett.* **12** 6000
[31] Schwab P M, Moosmann C, Wissert M D, Schmidt E W, Ilin K S, Siegel M, Lemmer U and Eisler H 2013 *Nano Lett.* **13** 1535
[32] Prodan E, Radloff C, Halas N J and Nordlander P 2003 *Science* **302** 419
[33] Talley C E, Jackson J B, Oubre C, Grady N K, Hollars C W, Lane S M, Huser T R, Norlander P and Halas N J 2005 *Nano Lett.* **5** 1569
[34] Thomas R and Swathi R S 2012 *J. Phys. Chem. C* **116** 21982
[35] Ou F S, Hu M, Naumov I, Kim A, Wu W, Bratkovsky A M, Li X M, Williams R S and Li Z Y 2011 *Nano Lett.* **11** 2538
[36] Palik E D 1984 *Handbook of Optical Constants of Solids* (Academic Press: New York)
[37] Jain P K, Huang W Y and EI-Sayed M A 2007 *Nano Lett.* **7** 2080
[38] Tanaka Y, Ishiguro H, Fujiwara H, Yokota Y, Ueno K, Misawa H and Sasaki K 2011 *Opt. Express* **19** 7726
[39] Sun Q, Ueno K, Yu H, Kubo A, Matsuo Y and Misawa H 2013 *Light: Sci. Appl.* **2** e118
[40] Atay T, Song J H and Nurmikko A V 2004 *Nano Lett.* **4** 1627
[41] Lassiter J B, Aizpurua J, Hernandez L I, Brandl D W, Romero I, Lal S, Hafner J H, Nordlander P and Halas N J 2008 *Nano Lett.* **8** 1212
[42] Almedia V R, Xu Q F, Barrios C A and Lipson M 2004 *Opt. Lett.* **29** 1209
[43] Kern J, Großmann S, Tarakina N V, Häckel T, Emmerling M, Kamp M, Huang J S, Biagioni P, Prangsma J C and Hecht B 2012 *Nano Lett.* **12** 5504
[44] Lim D K, Jeon K S, Kim H M, Nam J M and Suh Y D 2010 *Nat. Mater.* **9** 60
[45] Lee J H, Nam J M, Jeon K S, Lim D K, Kim H M, Kwon S, Lee H and Suh Y D 2012 *ACS Nano* **6** 9574
[46] Zuloaga J, Prodan E and Nordlander P 2009 *Nano Lett.* **9** 887
[47] Scholl J A, Garcia-Etxarri A, Koh A L and Dionne J A 2013 *Nano Lett.* **13** 564